Library Progress International *Print version ISSN 0970 1052*
Vol.44, No.4, Jul-Dec 2024: P. 666-672 *Online version ISSN 2320 317X*

Original Article *Available online at www.bpasjournals.com*

Deep Residual Networks: Transforming the Landscape of Image Recognition

Abhishek Pandey[1], Dr. V. Ramesh[2]

[1]PhD. Research Scholar, SCSVMV University, Kanchipuram (Tamil Nadu), Email: apandey.net@gmail.com
[2]Assistant Professor, SCSVMV University, Kanchipuram (Tamil Nadu), Email: rameshvpothy@gmail.com

How to cite this article: Abhishek Pandey, Dr. V. Ramesh (2024). Deep Residual Networks: Transforming the Landscape of Image Recognition. Library Progress International, 44(4), 666-672

Abstract
Background: For the categorization of Hyperspectral Images (HSI), deep learning-based integration of spectral-spatial statistics is becoming more and more popular. The Deep Residual Features Distilling Channels Attentiveness Network (DRFDCAN) represents a major improvement in medical imaging Super-Resolution (SR). One of the most prevalent conditions that may be first identified by visual inspection and then identified with the use of dermoscopic examination and further tests is skin cancer.
Aim: Examining the representations of feature that deep residual neural networks have learnt at various layers allows us to understand how they represent semantic ideas and hierarchical information in pictures.
Method: Visual observation, as in the beginning, provides the chance to use the power of AI to intercept the various skin images; thus, a number of deep learning techniques for skin lesion categorization that rely on Convolution Neural Networks (CNNs) and annotation skin images show more favourable results.
Results: Region of Interest (RoI) for skin lesions from dermoscopy photographs was segmented using Swarm Intelligence (SI) algorithms, and features of the RoI marked as the best separation result generated by the Grasshopper Optimizing Algorithm (GOA) were extracted using Speeded-Up Robustness Features (SURF).
Conclusion: Conclusions of the recommended segmentation as well as classification techniques are evaluated in terms of The F-measure, precision, the MCC, dice coefficients, the Jacquard index, sensitivity, specificity, and classification accuracy; on average, these metrics show 98.42 percent accuracy for classification, 97.73 percent preciseness, and 0.9704 percentages MCC.
Keywords: Convolution Neural Network (CNN), Deep Learning, Classification Techniques, Artificial Intelligence, Skin Cancer, Tests, Dermoscopic Analysis.

I. INTRODUCTION

Despite the use of non-intrusive techniques, comprehensive images of different bodily areas and organs can get created using CT and MRI machines. In medical practice, these pictures are often utilized to determine and treat problems ranging from internal bleeding to malignancies. A number of things, including the equipment's capacity, the surroundings, and expenses, might make the process of taking these pictures more difficult. Computer-aided systems and healthcare professionals' evaluations may be impacted by imprecise or poor-quality photographs. Certain abnormalities, such as micro aneurysms or haemorrhages, may occupy very small regions in images of the fundus of the eye [1]. Furthermore, some components—like soft exudates and certain growths—might not be apparent right away.

Thus, it is essential to increase the degree of detail of these medical care photographs. Making appropriate therapeutic judgments is greatly influenced by the quality presented in these clinical images [1, 2]. Optimizing the functioning of Computer-Aided Diagnosis (CAD) systems demands preliminary processing. It aids in raising contrast, lowering noise, and improving quality. One issue with medical imaging is the fact that Low Resolution (LR) images are often obtained because of equipment limitations and time restrictions during acquisition [3, 4]. Researchers have created a number of methods that enhance imagine clarity in order to get around issue. Creating a High-Resolution (HR) picture from its LR form generally the goal of SR.

Fortunately, leishmaniosis drug research could go through a radical change thanks to developments in Artificial Intelligence (AI) and machine learning. These tools may be used to forecast possible medication candidates and analyse large, intricate information sets. AI may hasten the search for leishmaniosis cures by lowering human error and offering a more focused and effective approach. It is important to highlight that there is still much to learn about the pathophysiology of leishmaniasis [5]. The creation of a leishmaniosis preventive vaccination is still a difficult job in spite of many attempts. Nonetheless, the use of AI along with deep learning algorithms has prompted the creation of a variety of analytical techniques, such as tools that are cognitive or in-silico based [5, 6]. These instruments may particularly create multiepitope vaccines based on immunoinformatics, which provide alternative vaccine candidates.

Preventing leishmaniosis requires rapid detection and timely treatment; yet, recurrent failures in traditional diagnostic procedures have caused delays in the initiation of chemotherapeutic and raised mortality rates in endemic regions. However, deep learning algorithms, a class of approaches that can identify complex patterns in large datasets, have shown state-of-the-art performance in several medical applications [7]. Deep learning is more accurate and adaptable than conventional machine learning techniques. For instance, a feature extractor strategy must be used initially in order for many machine learning approaches to interpret raw natural information, such as speech signals or images.

While early HSI classification algorithms mostly focused on spectral information, both spatial and spectral information are significant in HSI classification. In order to extract differentiating spectral characteristics, a variety of feature extraction techniques were put forward, neglecting the spatial connection between neighbouring pixels. Support Vector Machines (SVM), [8, 9], random forests, and their variations are samples of traditional classifiers. These approaches may not provide the complementing geographical knowledge, nonetheless. The targeted items' rich spatial structural information is made available by the high spatial resolution [10]. Techniques based on spatial characteristics were used, including the Gabor filter and the Gray Level Occurrence Matrix (GLCM).

For HSI classification, spectral-spatial analysis is now the predominant method. For example, Kang et al. optimized the SVM probability findings by using Edge Preserving Filtering (EPF) as a post-processing strategy. Moreover, techniques like composite kernels and morphological profiles made use of spectral and spatial data [11, 12]. In general, their performance for categorization of HSI is better than that of addresses that primarily depend on spectral characteristics.

Feature collection and classifying are the two main phases in the HSI classification algorithms listed above. They primarily concentrate on creating powerful feature images, however these crudely drawn features have limited ability to capture the wealth of spectral-spatial data and are unable to adequately capture the intricate nature of HISs [12, 13].

Deep learning has shown impressive results recently in a number of domains, including object identification, intelligent speech, picture segmentation, and medical imaging analysis. Deep learning techniques transformed HSI categorization by gaining access to high-level, semantic information. As a result, they are now a popular trend in HSI study. To extract high-level features, Autoencoders that are Stacked (SAEs) and its variations were used. For example, following feature dimensionality reduction, high-level features were extracted using stacked autoencoders.

Using a stacked scant auto-encoder network, the redundancy issue with high-dimensional data was resolved without the need for dimensionality reduction by simply learning an insufficient sparse spectrum representation of feature from the original hyperspectral data set. Ma et al. suggested a spatial updated deep autoencoder, an enhanced SAE, [13, 14], for gathering spectral-spatial knowledge by updating the features while taking contextual information into account. Additionally, confirmed that Deep Belief Networks (DBN) are eligible with regard to HSI spectral-spatial assessment [15].

These approaches include learning-based algorithms, restoration, and interpolation. Deep learning algorithms have emerged as a major breakthrough recently, showing promise in several medical imaging domains while maintaining critical features. Neural network-based Single Image Super-Resolution (SISR) approaches have surpassed previous approaches such as interpolation-based, reconstruction-based, [16], and training-based methods on natural pictures due to the progress made in deep learning algorithms. It is still difficult to modify deep neural networks for improved resolution in medical imaging. The improved pictures are used for medical evaluation in clinical settings, however the amount of the datasets that are readily accessible is often restricted.

Therefore, new methods for improving the resolution in medical imaging are required. This involves making changes to assessment measures, training datasets, loss functions, and neural network designs in order to highlight significant frameworks and maintain important features for medical specialists. The resolution of medical pictures has lately showed promise for CNNs and Generational Adversarial Networks (GANs). However, there is more work to be done on Vision Integrating Transformers (ViTs), despite their superior performance in organic imagine improving and medical image analysis.

Examining the benefits, possibilities, efficacy, and drawbacks when employing ViTs for medical imaging SR is crucial. Furthermore, integrated CNN-ViT models may benefit from the addition of well-known CNN design strategies such as feature blending, residual linkages, and localization procedures. For instance, a modified ViT called as the Swain Transformer has been created for advanced image tasks, leveraging on common weights and localization features of CNNs. These novel Swin layers are being used to natural imagery segmentation and refining applications.

SR efforts may be enhanced by using previous knowledge from similar medical imaging tasks, such as segmentation. On the one hand, challenges still exist when evaluating the quality of improved photographs, especially in the medical field [16, 17]. Restoration accuracy and human understanding are often evaluated as part of the improved natural imagine quality evaluation procedure. As SISR addresses approach the limits of signal fidelity the measurements, perceptual evaluations of quality have become of greater significance.

However, there are particular difficulties with medical photos, since the patient's mobility and the hardware of the imaging system are the main causes of artefacts, which are uncommon in natural photographs. In medical image SR research, Including Metrics as PSNR and Structural Similarity (SSIM) are often used. However, using qualitative assessment methods designed for natural photos only may not be reliable for medical SR activities. In addition, researchers often evaluate the quality of improved pictures by seeing how well they perform in other medical image analysis tasks, such as segmentation. Medical practitioners unquestionably want high-quality images for accurate diagnosis, even if measurement standards are not directly correlated to diagnostic accuracy. Similar to current perceptual loss strategies, previously acquired information from previous methods of segmentation may also help optimize medical SR models, beyond merely machine-based quality requirements.

To find any indication that a skin lesion is developing into melanoma, the ABCDE rule—a primary skin examination—should be used. Dermoscopy is a harmless skin scanning technique that improves the detection of cancer by producing a brightly lighted, enlarged picture of a skin slice. Melanoma is often diagnosed via dermoscopy, which is significantly more reliable than a visual evaluation. Asymmetry, which indicates that the two portions of the lesion ought not to coincide particularly the case of a malignant lesion, is one amongst the warning indicators for the disease. According to study B (Border), the majority of melanoma cases have rough surfaces and notchy margins. A danger indicator is indicated by C (Color), which denotes that the mole is displaying numerous colours, such as red, blue, or brown. The letter D (Diameter/Dark) represents a larger and deeper hue of melanoma lesions. Colorless amelanotic melanoma is an uncommon observation. E (Evolving) denotes any change in the skin lesion's size, colur, and texture that might or might not cause it to pain or bleed, since those modifications signal a step closer to fatality.

1.1 Objectives of the study

- Measuring the accuracy, speed, and durability of deep residual networks by analysing their performance on a range of image identification applications, including datasets from benchmarks like ImageNet.
- Examining deep residual networks' training dynamics, such as their sensitivity to hyper parameters, speed of convergence, and optimization difficulties, in order to understand how they behave during learning.
- Investigating deep residual networks' efficiency and scalability in terms of model size, computing power, and memory footprint to determine whether or not they can be used for applications involving large amounts of data and resource-constrained devices.

II. LITERATURE REVIEW

(Xue, Z., Yu, X., 2021) [18] In order to enhance the performance of traditional deep learning networks, this paper presents a unique Hierarchical residual network with Attention Mechanism (HResNetAM) for Hyperspectral Imaging (HSI) spectral-spatial classification. Handling with the highly dimensional nonlinear behaviours seen in HSIs requires using the multiscale spatial and spectral aspects that are not easily exploited by the simple convolutional neuronal network-based models. The suggested hierarchical residual network could extract multiscale spatially and spectral characteristics at an individual level, expanding its receptive fields range and improving the model's capacity for representing features.

(Krishna, V., 2019) [19] Deep learning has been transforming the way robots receive and comprehend visual information in the area of image identification in recent years. This work sheds light on the extraordinary advances and difficulties in this dynamic subject by providing an extensive assessment of the various architectures and approaches used in Deep learning has been for the recognition of images. The first section of the study offers a thorough synopsis of the basic ideas behind the use of deep learning for image identification. From the first Convolutional Neural Networks (CNNs) to more complex models like Residual Network (ResNets), inception networks, and attention processes, it explores the development of neural network designs. Each architecture is broken further to show its advantages, disadvantages, and the specific image recognition assignments that it does well.

(Anteby, R., Horesh, N., 2021) [20] Deep learning has completely changed medical image processing in the last ten years. This method might improve laparoscopic procedures. The aim of the study was to assess the accuracy with which deep learning networks can analyse footage of laparoscopic surgeries. We searched the databases of Medline, Embase, an IEEE Explore, and the International Journal of Sciences between January 2012 and May 5, 2020. A few research examined the use of convolutional neural networks, also known as a deep learning model, for laparoscopic surgery video analysis. The study's attributes, such as the source of the dataset, the method of operation, the quantity of videos, and the prediction application, were contrasted.

(Zhu, G., Jiang, B., 2019) [21] Numerous deep learning-based clinical applications related to radiography have been suggested and investigated. These applications include risk assessment, separation tasks, prognosis and diagnosis, and even therapeutic response prediction. Numerous other leading-edge uses of AI exist in the technical fields of medical imaging, especially when it comes to image acquisition. These uses include the elimination of image artefacts, the normalization and harmonisation of images, the enhancement of image quality, the reduction of irradiation and contrast dosage, and the abbreviation of imaging study duration. This piece will discuss the subject and attempt to provide a synopsis of deep learning methods used in neuroscience.

(Tiulpin, A., 2020) [22] The most prevalent musculoskeletal condition worldwide is Osteoarthritis (OA) of the knee. In general medicine, radiographic evaluation and physical inspection are used to diagnose knee OA. An impartial assessment of knee osteophytes, joint space narrowing, and additional knee attributes may be carried out using the Osteoarthritis Research Society International (OARSI) atlas of OA radiographic findings. This offers a deeper assessment of the knee's OA symptoms than the widely accepted and highly regarded Kellgren–Lawrence (KL) composite score. In this work, we created an automated technique to use knee radiographs to predict KL and OARSI grade. Our approach employs an ensemble of 50-layer residual networks and is based on deep learning. We used fine-tuning and transfer learning using ImageNet to the Osteoporosis Initiative (OAI) dataset.

(Huang, S. C., Shen, L., 2021) [23] Radiologists have a constantly expanding workload due to the surge in medical imaging tests in recent years. Clinical guidance in decisions and autonomous medical picture analysis have a potential new tool in deep learning. Obtaining large-scale manually annotated datasets for medical photos is a challenging and costly task when it comes to training deep neural networks. The goal of this effort is to use radiology reports to create multi-modal medical imaging representations that are label-efficient. In particular, we recommend utilizing the paired report's picture sub-regions and words to contrast in order to teach learners both Global and Local Representation utilizing our Attention-based Architecture (GLoRIA).

III. METHODS

Using dermoscopic pictures, the authors of this study newspaper developed an intelligent classification model and an autonomous skin lesion segmentation system [24]. Here, we combined the Convolutional Neural Network (CNN) with the swarm-based Grasshopper Optimization Algorithm (GOA) as a machine learning technique.

3.1 Proposed Method

An automated skin cancer segmentation and intelligence classification algorithms were created using the mentioned data sets, and Figure 1 illustrates the general procedure of the suggested approach. The whole operational process of the proposed model illustrates the module's functioning architecture, which helps with the separation and categorization of skin cancers from dermoscopic images of lesions in the skin [25].

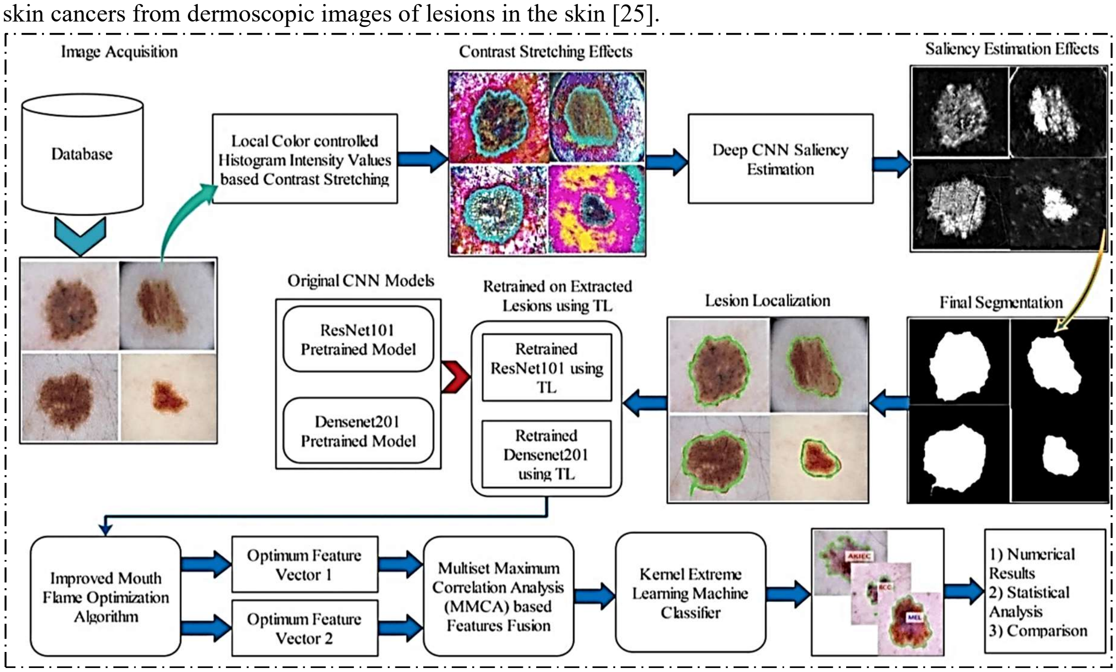

Fig. 1 Method of intelligent classification model and automated segmenting of skin lesions.

Table 1 shows the entropy calculations for a mask modification of {1: 3} % incremental improve as a point of comparison [25].

Table 3 Entropy of the processed and initial images.

Proportion of Entropy for Mask Fluctuation	Original Entropy	Entropy proposed	% differences
10	7.89522	6.149563	14.589
12	7.14926	6.479855	10.60895
16	7.59871	6.249561	14.14589
18	7.14982	6.148592	21.41658
20	7.65952	6.589526	14.59788
22	7.89564	6.258966	3.598660
24	7.72622	6.528963	12.48962

IV. RESULT AND DISCUSSION

The present section uses three distinct data sets to analyse the output of the intelligent classification model and the predicted computerized skin lesion segment [26, 27]. Table 2 represents the total number of photos that the projected model utilized for skin lesion dermoscopic imaging segmentation and categorization.

Table 2 Data set definition for intelligent model for classification and automated skin lesion segmentation.

Class	**ISIC-2018**		**PH-2**		**ISIC-2017**	
	Training	**Testing**	**Training**	**Testing**	**Training**	**Testing**
Melanoma	700	1000	500	400	600	1200
No melanoma	700	1000	500	400	600	1200

$\mathrm{CA} = \frac{\mathrm{TP+TN}}{\mathrm{TP+TN+FP+F}}$ ………1

$\mathrm{precision} = \frac{\mathrm{TP}}{\mathrm{TP+FP}}$ ……….2

$\mathrm{Sensitivity} = \frac{\mathrm{TP}}{\mathrm{TP+FN}}$ ……….3

$\mathrm{F_1} = 2.\frac{\mathrm{precision.sensitivity}}{\mathrm{precision+sensitivit}}$ ………4

$\mathrm{MCC} = \frac{(\mathrm{T_P \times T_N}) - (\mathrm{F_P \times F_N})}{\sqrt{\mathrm{T_P+F_P}) + (\mathrm{T_P+F_N}) + (\mathrm{T_N+F_P}) + (\mathrm{T_N+F_N})}}$ …….5

$\mathrm{DSC} = \frac{2\mathrm{T_P}}{2\mathrm{T_N}+\mathrm{F_P}+\mathrm{F_N}}$. …….6

$\mathrm{Jaccard} = \frac{\mathrm{T_P}}{\mathrm{T_P+F_P+F_N}}$. ……7

The average precision comparisons for K-means with all three of these algorithms is shown in Table 3 below, [28, 29], confirming the efficacy of GOA for skin lesion dermoscopic images.

Table 3 Segmentation accuracy-based comparison of K-mean with PSO, the FFA, or GOA.

No. of Images	**k-means**	**k-means with PSO**	**K-means with FFA**	**K-means with GOA**
100	45.18	78.45	64.85	94.58
200	25.64	24.58	24.96	98.62
300	69.52	68.98	89.41	95.64
400	67.98	28.48	78.98	97.56
500	25.78	25.98	54.86	94.85
600	69.57	68.98	62.89	96.18
700	54.89	27.89	14.58	96.78
800	68.95	67.86	97.65	98.96
900	67.89	89.25	62.59	96.15
1000	58.79	36.59	48.96	97.68

4.1 Evaluation of Performance Against Various Data Sets

For 1000 picture samples, it calculates the parametric value of many parameters utilized for the performance study of the proposed work utilizing three separate data sets—PH2, [30], explained in Table 8.

Table 4 The model's effectiveness is assessed using the PH-2 data set.

Samples	**Accuracy (%)**	**Sensitivity**	**Precision**	**MCC**	**Dice**	**Jacquard**	**Specificity**
100	98.596	0.8964	0.9687	0.9648	0.4189	0.6985	0.8965
200	96.485	0.5896	0.8964	0.7956	0.9516	0.8814	0.9756

300	95.846	0.1478	0.8649	0.8945	0.2896	0.9648	0.9482
400	93.486	0.1495	0.8614	0.5169	0.9761	0.9896	0.9615
500	98.640	0.5895	0.5268	0.8612	0.9861	0.9845	0.9876
600	98.679	0.5298	0.8976	0.5892	0.1488	0.9614	0.9614
Average	96.478	0.8675	0.6489	0.8961	0.5269	0.9658	0.9786

V. CONCLUSION

Super-resolution methods have advanced significantly, particularly in the field of medical imaging. The importance of image resolution for healthcare evaluations demands technologies that strike a compromise between computing efficiency and clarity. Despite their potential, conventional ones CNN-based SR algorithms struggle with computational limitations, especially on devices with constrained resources. Evaluating the efficiency of the most recent RFDN model. With the use of CNN-based computer-assisted diagnostic systems, which use a deep learning technique that automatically separate features from patterns for effective categorization, dermoscopy pictures are accessible to assist in the identification of skin lesions. This research identified photos of skin lesions using the ISIC-2017, ISIC, or the-2018, and pH-2 data sets. The model achieved a 98.42% rate of classification accuracy.

In order to do this, a variety of presently accessible SI approaches are assessed, and it is discovered that GOA performs the best for dividing skin lesions job. Additionally, CNN is used to classify skin cancer images into melanoma and no melanoma classes and SURF is used to extract features from segmented areas. With 98.42% success rate in classification, 97.73% precision, and an MCC of 0.9704, the suggested work performs appropriate and outperforms the previous work by 6.12% accurate. The suggested method outperforms the current work with greater specificity, perfection, and F-measure of 9.21%, 5.78%, and 8.34%, respectively.

FUTURE WORKS

Increased performance may be achieved in future studies by improving the model, updating the data set, and further assessing for additional classes to meet the actual-life difficulties in identifying and treating conditions.

VI. REFERENCES

1. S. Burza, S. L. Croft, and M. Boelaert, “Leishmaniasis—authors’ reply,” The Lancet, vol. 393, no. 10174, pp. 872-873, 2019.
2. D. Kumari, S. Perveen, R. Sharma, and K. Singh, “Advancement in leishmaniasis diagnosis and therapeutics: an update,” European Journal of Pharmacology, vol. 910, Article ID 174436, 2021.
3. E. K. Elmahallawy, A. Sampedro Martinez, J. Rodriguez-Granger et al., “Diagnosis of leishmaniasis,” The Journal of Infection in Developing Countries, vol. 8, no. 8, pp. 961–972, 2014.
4. R. C. F. De Brito, R. D. de O. Aguiar-Soares, J. M. de O. Cardoso, W. Coura-Vital, B. M. Roatt, and A. B. Reis, “Recent advances and new strategies in Leishmaniasis diagnosis,” Applied Microbiology and Biotechnology, vol. 104, no. 19, pp. 8105–8116, 2020.
5. S. Pund and A. Joshi, “Nanoarchitectures for neglected tropical protozoal diseases: challenges and state of the art,” in Nano- and Microscale Drug Delivery Systems, A. M. Grumezescu, Ed., pp. 439–480, Elsevier, 2017.
6. T. P. C. Dorlo, M. Balasegaram, J. H. Beijnen, and P. J. de Vries, “Miltefosine: a review of its pharmacology and therapeutic efficacy in the treatment of leishmaniasis,” Journal of Antimicrobial Chemotherapy, vol. 67, no. 11, pp. 2576–2597, 2012.
7. A. Ponte-Sucre, F. Gamarro, J.-C. Dujardin et al., “Drug resistance and treatment failure in leishmaniasis: a 21st century challenge,” PLOS Neglected Tropical Diseases, vol. 11, no. 12, Article ID e0006052, 2017.
8. Zhao, G.; Wang, X.; Kong, Y.; Cheng, Y. Spectral-Spatial Joint Classification of Hyperspectral Image Based on Broad Learning System. Remote Sens. 2021, 13, 583.
9. Li, S.; Song, W.; Fang, L.; Chen, Y.; Ghamisi, P.; Benediktsson, J.A. Deep learning for hyperspectral image classification: An overview. IEEE Trans. Geosci. Remote Sens. 2019, 57, 6690–6709.
10. Fang, B.; Li, Y.; Zhang, H.; Chan, J.C.W. Hyperspectral images classification based on dense convolutional networks with spectral-wise attention mechanism. Remote Sens. 2019, 11, 159.
11. Xing, Z.; Zhou, M.; Castrodad, A.; Sapiro, G.; Carin, L. Dictionary learning for noisy and incomplete hyperspectral images. SIAM J. Imaging Sci. 2012, 5, 33–56.
12. Zhang, Y.; Cao, G.; Li, X.; Wang, B. Cascaded random forest for hyperspectral image classification. IEEE J. Sel. Top. Appl. Earth Obs. Remote Sens. 2018, 11, 1082–1094.
13. Jain, D.K.; Dubey, S.B.; Choubey, R.K.; Sinhal, A.; Arjaria, S.K.; Jain, A.; Wang, H. An approach for hyperspectral image classification by optimizing SVM using self-organizing map. J. Comput. Sci. 2018, 25, 252–259.

14. Huang, Y.; Zhang, C.; Su, W.; Yue, A. A Study of the optimal scale texture analysis for remote sensing image classification. Remote Sens. Land Resour. 2008, 4, 14–17.
15. Yan, Y.; Liu, R.; Chen, H.; Zhang, L.; Zhang, Q. CCT-Unet: A U-shaped Network based on Convolution Coupled Transformer for Segmentation of Peripheral and Transition Zones in Prostate MRI. IEEE J. Biomed. Health Inform. 2023, 27, 4341–4351.
16. Kastryulin, S.; Zakirov, J.; Pezzotti, N.; Dylov, D.V. Image quality assessment for magnetic resonance imaging. IEEE Access 2023, 11, 14154–14168.
17. Kelkar, V.A.; Gotsis, D.S.; Brooks, F.J.; Prabhat, K.C.; Myers, K.J.; Zeng, R.; Anastasio, M.A. Assessing the ability of generative adversarial networks to learn canonical medical image statistics. IEEE Trans. Med. Imaging 2023, 42, 1799–1808.
18. Güven, S.A.; Talu, M.F. Brain MRI high resolution image creation and segmentation with the new GAN method. Biomed. Signal Process. Control 2023, 80, 104246.
19. Xue, Z., Yu, X., Liu, B., Tan, X., & Wei, X. (2021). HResNetAM: Hierarchical residual network with attention mechanism for hyperspectral image classification. IEEE Journal of Selected Topics in Applied Earth Observations and Remote Sensing, 14, 3566-3580.
20. Krishna, V., Singh, A., & Gupta, D. (2019). Deep learning for image recognition: A survey of architectures and techniques.
21. Anteby, R., Horesh, N., Soffer, S., Zager, Y., Barash, Y., Amiel, I., ... & Klang, E. (2021). Deep learning visual analysis in laparoscopic surgery: a systematic review and diagnostic test accuracy meta-analysis. Surgical Endoscopy, 35, 1521-1533.
22. Zhu, G., Jiang, B., Tong, L., Xie, Y., Zaharchuk, G., & Wintermark, M. (2019). Applications of deep learning to neuro-imaging techniques. Frontiers in neurology, 10, 869.
23. Tiulpin, A., & Saarakkala, S. (2020). Automatic grading of individual knee osteoarthritis features in plain radiographs using deep convolutional neural networks. Diagnostics, 10(11), 932.
24. Huang, S. C., Shen, L., Lungren, M. P., & Yeung, S. (2021). Gloria: A multimodal global-local representation learning framework for label-efficient medical image recognition. In Proceedings of the IEEE/CVF International Conference on Computer Vision (pp. 3942-3951).
25. D. N. H. Thanh, V. B. Prasath, L. M. Hieu, and N. N. Hien, "Melanoma skin cancer detection method based on adaptive principal curvature, colour normalisation and feature extraction with the ABCD Rule," Journal of Digital Imaging, vol. 3, pp. 1–12, 2019.
26. B. Prasanalakshmi, K. Murugan, K. Srinivasan, S. Shridevi, S. Shamsudheen, and Y.-C. Hu, "Improved authentication and computation of medical data transmission in the secure IoT using hyper elliptic curve cryptography," The Journal of Supercomputing, vol. 78, no. 1, pp. 361–378, 2022.
27. G. S. Sriram, "Edge computing vs. Cloud computing: an overview of big data challenges and opportunities for large enterprises," International Research Journal of Modernization in Engineering Technology and Science, vol. 4, no. 1, pp. 1331–1337, 2022.
28. G. S. Sriram, "Security challenges of big data computing," International Research Journal of Modernization in Engineering Technology and Science, vol. 4, no. 1, pp. 1164–1171, 2022.
29. M. A. Khan, M. Sharif, T. Akram, R. Damaševičius, and R. Maskeliūnas, "Skin lesion segmentation and multiclass classification using deep learning features and improved moth flame optimization," Diagnostics, vol. 11, no. 5, p. 811, 2021.
30. S. Jinnai, N. Yamazaki, Y. Hirano, Y. Sugawara, Y. Ohe, and R. Hama moto, "The development of a skin cancer classification system for pigmented skin lesions using deep learning," Biomolecules, vol. 10, no. 8, p. 1123, 2020.